Sr^{2+}/Ca^{2+} and $^{44}Ca/^{40}Ca$ fractionation during inorganic calcite formation: III. Impact of salinity/ionic strength

Jianwu Tang, Andrea Niedermayr, Stephan J. Köhler, Florian Böhm, Basak Kısakürek,

Anton Eisenhauer, and Martin Dietzel

Preprint

Sr^{2+}/Ca^{2+} and $^{44}Ca/^{40}Ca$ fractionation during inorganic calcite formation: III. Impact of salinity/ionic strength

Jianwu Tang[1,*], Andrea Niedermayr[1], Stephan J. Köhler[2], Florian Böhm[3], Basak Kısakürek[3], Anton Eisenhauer[3], and Martin Dietzel[1]

[1]Institute of Applied Geosciences, Graz University of Technology, Rechbauerstrasse 12, A-8010 Graz, Austria
[2]Department of Aquatic Sciences and Assessment, P.O. Box 7050, SE-75007 Uppsala, Sweden
[3]Leibniz-Institut für Meereswissenschaften, IFM-GEOMAR, Wischhofstr. 1-3, D-24148 Kiel, Germany

*Corresponding author. Present address: Department of Earth & Environmental Sciences, Tulane University, 6823 St. Charles Avenue, New Orleans, LA 70118, USA. *E-mail address*: jtang@tulane.edu

43   **Abstract**

44   In order to apply Sr/Ca and ^{44}Ca/^{40}Ca fractionation during calcium carbonate ($CaCO_3$) formation

45   as a proxy to reconstruct paleo-environments, it is essential to evaluate the impact of various

46   environmental factors. In this study, a CO_2 diffusion technique was used to crystallize inorganic

47   calcite from aqueous solutions at different ionic strength/salinity by the addition of NaCl at 25°C.

48   Results show that the discrimination of Sr^{2+} versus Ca^{2+} during calcite formation is mainly

49   controlled by precipitation rate (R in $\mu mol/m^2/h$) and is weakly influenced by ionic

50   strength/salinity. In analogy to Sr incorporation, ^{44}Ca/^{40}Ca fractionation during precipitation of

51   calcite is weakly influenced by ionic strength/salinity too. At 25°C the calcium isotope

52   fractionation between calcite and aqueous calcium ions ($\Delta^{44/40}Ca_{calcite-aq} = \delta^{44/40}Ca_{calcite} -$

53    $\delta^{44/40}Ca_{aq}$) correlates inversely to log R values for all experiments. In addition, an inverse

54   relationship between $\Delta^{44/40}Ca_{calcite-aq}$ and log D_{Sr}, which is independent of temperature,

55   precipitation rate, and aqueous $(Sr/Ca)_{aq}$ ratio, is not affected by ionic strength/salinity either.

56   Considering the log D_{Sr} and $\Delta^{44/40}Ca_{calcite-aq}$ relationship, Sr/Ca and $\delta^{44/40}Ca_{calcite}$ values of

57   precipitated calcite can be used as an excellent multi-proxy approach to reconstruct

58   environmental conditions (e.g., temperature, precipitation rate) of calcite growth and diagenetic

59   alteration.

60

1. Introduction

Trace and minor metal ratios (e.g., Sr/Ca and Mg/Ca) and stable isotope ratios (e.g., $^{18}O/^{16}O$ and $^{44}Ca/^{40}Ca$) in biogenic $CaCO_3$ have been widely used to estimate past sea surface temperatures (SST; e.g. Rostek et al., 1993; Elderfield and Ganssen, 2000; Gussone et al., 2004; Barker et al., 2005; Corrège, 2006). In addition, it is commonly accepted that the oxygen isotope ratio ($^{18}O/^{16}O$) in biogenic calcium carbonates is a function of salinity of the solution from which calcium carbonates were grown. Thus, combined with other chemical or isotopic indicators, $^{18}O/^{16}O$ ratios in biogenic calcium carbonates can also be used as a proxy for past sea surface salinity (SSS; e.g. Eisma et al., 1976; Rostek et al., 1993; Gussone et al., 2004; Sampei et al., 2005; Corrège, 2006).

Until now, only a few studies have examined the effect of salinity on $^{44}Ca/^{40}Ca$ ratios in biogenic calcium carbonates. The calcium isotopic composition of *Thoracosphaera heimii* (dinoflagellate) cysts was found to have no significant correlation with salinity (Gussone et al., 2010), whereas that of the planktic foraminifer, *Globigerinoides ruber*, was observed to have a negative linear correlation presumably due to a growth rate effect (Kısakürek et al., 2011).

The magnitude of salinity influence on Sr/Ca or Mg/Ca ratios in biogenic calcium carbonates remains disputed. Some studies (e.g., Eisma et al., 1976; Rosales et al., 2004) suggest a negligible salinity effect on Sr/Ca and/or Mg/Ca ratios in molluscs, whereas others (e.g., Klein et al., 1996; Nürnberg et al., 1996; Lea et al., 1999; Ferguson et al., 2008; Kısakürek et al., 2008, 2011; Dissard et al., 2010) postulate either a noticeable or a strong salinity effect on Sr/Ca and/or Mg/Ca ratios in mollusks and foraminifera. Additional studies (e.g., Dueñas-Bohórquez et al., 2009) indicate that salinity only influences Mg/Ca ratios but not Sr/Ca ratios in cultured planktonic foraminifera. The high Mg/Ca ratios of planktic foraminifera in high salinity

84 environments were observed to be associated with early diagenetic effects through the

85 precipitation of high-Mg-calcite overgrowths rather than physiological uptake (Hoogakker et al.,

86 2009). However, foraminifera from the Atlantic coretop samples of Arbuszewski et al. (2010)

87 have no diagenetic coatings but still show a clear salinity effect on Mg/Ca ratios. Thus,

88 Arbuszewski et al. (2010) concluded that diagenetic overgrowth mechanism suggested by

89 Hoogakker et al. (2009) for the high Mg/Ca ratios of foraminifera at high salinity was not

90 applicable to their samples taken from open Atlantic Ocean.

91   Metabolic mechanisms may overprint mineralogical salinity effects on trace element

92 incorporation in biogenic carbonates. However, even in inorganic precipitation experiments, the

93 extent to which salinity influences Sr/Ca ratios of calcium carbonate crystals is also still under

94 debate. Some studies (e.g., Holland et al., 1963, 1964; Katz et al., 1972; Gaetani and Cohen,

95 2006) indicate that Sr/Ca ratios in inorganic calcium carbonates are insensitive to variations in

96 salinity. Holland et al. (1963, 1964) reported that, at temperatures between 90º and 100ºC, the

97 Sr/Ca ratio in aragonite was essentially constant when NaCl concentrations varied from 36.2 to

98 3640 mM, and the Sr/Ca ratio in calcite was essentially independent of NaCl concentrations up

99 to 1400 mM. In contrast, the experimental results of Pingitore and Eastman (1986) imply a

100 significant decrease of Sr/Ca ratios in calcite with increasing salinity. They reported that Sr

101 distribution coefficients (i.e., their partition coefficient k_{Sr}) ranged from 0.10 to 0.19 without

102 NaCl in the growth solutions of calcite but from 0.04 to 0.06 with 480 mM NaCl in the growth

103 solutions. Thus, the presence of dissolved NaCl significantly lowered the Sr/Ca ratio in calcite.

104 Pingitore and Eastman (1986) proposed a multiple site model and argued that the depression of

105 Sr partitioning in the presence of NaCl might be due to competition between Na^+ and Sr^{2+} for

106 non-lattice sites. Although values for respective precipitation rates are not given in Pingitore and

107 Eastman (1986) as in most of the other studies, their experiments indicated that fast precipitation

108 resulted in more Sr partitioning into calcite. The multiple site model was again proposed by

109 Pingitore and Eastman (1986) as a possible cause of rate effect on Sr partitioning. They

110 suggested that non-lattice sites probably were related to site defects with preferential

111 incorporation of larger cations (such as Sr^{2+}) than Ca^{2+}. Fast precipitation results in more crystal

112 defects and thus a larger partition coefficient k_{Sr}.

113   It is not a trivial task to constrain the impact of ionic strength on Sr/Ca and $^{44}Ca/^{40}Ca$

114 fractionation during inorganic calcium carbonate formation. If no ionic strength effect is

115 identified on Sr/Ca and $^{44}Ca/^{40}Ca$ ratios, both may be used as potential proxies for past SST and

116 to isolate temperature and salinity effects on $^{18}O/^{16}O$ ratio in inorganic calcium carbonates. If a

117 salinity effect does exist, Sr/Ca and $^{44}Ca/^{40}Ca$ ratios can be calibrated by salinity, and may be

118 used to trace past SSS. However, in any of the tasks above special attention has to be given to

119 precipitation rate, as a strong rate impact on Sr incorporation and calcium isotope fractionation

120 during inorganic calcite precipitation is known from previous studies (e.g. Lorens, 1981;

121 Tesoriero and Pankow, 1996; Lemarchand et al., 2004; Tang et al., 2008a, b).

122   In our previous studies (Tang et al., 2008a, b), the effect of temperature and precipitation

123 rate on Sr/Ca and $^{44}Ca/^{40}Ca$ fractionation was investigated and the possibility to use Sr/Ca and

124 $^{44}Ca/^{40}Ca$ fractionation as a multi-proxy to decipher calcite precipitation conditions was

125 discussed. In this study, inorganic calcite was precipitated from aqueous solutions at different

126 ionic strength/salinity by the addition of NaCl. Our purpose was to investigate the impact of

127 salinity/ionic strength on Sr/Ca and $^{44}Ca/^{40}Ca$ fractionation during the precipitation of inorganic

128 calcite at well-known physicochemical conditions and precipitation rates.

129   **2. METHODS**

130   All experiments were conducted at room temperature (25°±0.5°C) in a temperature-

131   controlled laboratory or a water bath. The chemicals used in our experiments, $CaCl_2 \cdot 2H_2O$,

132     $SrCl_2 \cdot 6H_2O$, NaCl, NaOH, $NaHCO_3$, and NH_4Cl (Merck), were reagent grade. Deionized water

133   (18.2 MΩ·cm, ELGA PURELAB Maxima) was used to prepare aqueous solutions. Values of pH

134   were measured by a pH combination electrode (SCHOTT Blue Line 28 pH Pt 1000), calibrated

135   at 25°C with NIST certified buffer solutions (pH 4.01, 7.00, and 10.00). Calcite was grown from

136   10 mM $CaCl_2$ + 5 mM NH_4Cl + 0.1 mM $SrCl_2$ background solution. Although two experiments

137   (Experiments # 12 and #13 in Table 1) were conducted without Sr addition, about 0.7 μM of Sr

138   in the growth solution was still observed by ICP-OES analyses due to the Sr content of the

139   reagent grade $CaCl_2 \cdot 2H_2O$ used in our experiments. In order to investigate the effect of

140   salinity/ionic strength on Sr/Ca and $^{44}Ca/^{40}Ca$ fractionation in calcite, precipitation experiments

141   were conducted with (1) background solution; (2) background solution + 257 mM NaCl; and (3)

142   background solution + 797 mM NaCl.

143   A CO_2-diffusion technique was used to spontaneously precipitate inorganic calcite from

144   the experimental solutions. Experimental setup has been described in detail in our previous study

145   (Tang et al., 2008a). Briefly, a polyethylene (PE) bottle containing 0.5 L of 0.83 M $NaHCO_3$

146   solution was soaked in a vessel containing 5 L of the growth solution (background solution with

147   NaCl as described above). According to Dietzel et al. (2004), PE membrane allows CO_2

148   diffusion from the $NaHCO_3$ solution to the growth solution, but prevents any cation diffusion

149   from the growth solution to the $NaHCO_3$ solution and vice versa. Thus, calcite precipitation only

150   occurs in the growth solution. The pH of the growth solution is kept constant at 8.30 by

151   automatic pH-stat titration with an accuracy of ±0.03 (Schott TitroLine alpha plus). To assure a

152   homogeneous solution for calcite growth, the growth solution was stirred at 200 rpm using a

6

153   floating stir bar (NALGENE® Labware, DS6630-4000). The precipitation rate of calcite was

154   controlled by adjusting the flux of CO_2 by changing the pH of the $NaHCO_3$ solution and/or the

155   thickness of PE membrane.

156   Formation of calcite as a single $CaCO_3$ polymorph was verified using X-Ray diffraction

157   (XRD, goniometer type Philips PW 1130/1370), Infrared Spectroscopy (FTIR, Perkin Elmer

158   1600), Micro Raman Spectroscopy (LABRAM HR-800UV), and imaging by scanning electron

159   microscopy (SEM, ZEISS Ultra 55). Typical FT-IR spectra and FT-Raman spectra of calcite

160   grown from our CO_2-diffusion technique were presented in Tang et al. (2008a). All calcite

161   precipitates of our experiments exhibit typical rhombohedral habit (Fig. 1). Precipitation rates (R)

162   were calculated from the amount of calcite precipitated, growth time, and specific surface area.

163   Specific surface area was estimated from particle size distribution of the final solid phase with a

164   centrifugal particle size analyzer (SHIMADZU SA-CP2). Typical cumulative particle size

165   distribution curves and the data about specific surface area of calcite as a function of growth time

166   were also presented in Tang et al. (2008a). The reader is referred to Tang et al. (2008a) for more

167   details about the procedure to estimate precipitation rate.

168   During each experiment, the chemical evolution of the growth solution was monitored by

169   ICP-OES (Perkin Elmer Optima 4300DV) measurement of small volumes (5 ml) of the growth

170   solution, sampled at specific time intervals. Because calcite crystals grown from our experiments

171   are tiny (particle size less than 50 μm), an aliquot (about 10 mg) of well-mixed solid calcite

172   crystals was sufficient for determining the cation composition of precipitated calcite. Thus, in

173   our studies, about 10 mg of solid calcite crystals from each experiment was dissolved into 20 ml

174   of 2% bidistilled HNO_3 solution and the digestion solution was analyzed by ICP-OES.

175   In this study, the Sr/Ca fractionation between calcite and solution is expressed as a Sr

176   distribution coefficient according to the equation

177    $$D_{Sr} = \left(\frac{[Sr]}{[Ca]}\right)_{calcite} \bigg/ \left(\frac{[Sr]}{[Ca]}\right)_{aq} \tag{1}$$

178   where $([Sr]/[Ca])_{calcite}$ is the molar Sr/Ca ratio of precipitated calcite and $([Sr]/[Ca])_{aq}$ is the

179   molar Sr/Ca ratio of the growth solution. Apparent D_{Sr} value for each experiment was estimated

180   from the composition of initial and final growth solution and cation content of precipitated

181   calcite. On average, Ca and Sr concentrations decreased by 10% and 2 % , respectively, during

182   the experiments.The overall evolution of the Sr distribution of the bulk calcite can be described

183   by the expression (Usdowski (1975)

184    $$\left(\frac{[Sr]}{[Ca]}\right)_{bulk\ calcite} = \left(\frac{[Sr]}{[Ca]}\right)_{aq,o} \cdot \frac{1 - \left(\frac{[Ca]}{[Ca]_o}\right)_{aq}^{D_{Sr}}}{1 - \left(\frac{[Ca]}{[Ca]_o}\right)_{aq}} \tag{2}$$

185   where $([Sr]/[Ca])_{bulk\ calcite}$ is the Sr/Ca molar ratio in the bulk calcite, $([Sr]/[Ca])_{aq,o}$ is the initial

186   Sr/Ca molar ratio in the aqueous solution before calcite precipitation, and $([Ca]/[Ca]_o)_{aq}$ is the

187   molar concentration ratio of aqueous Ca to the initial aqueous Ca (Tang et al. 2008a for more

188   details about the estimation of D_{Sr} values) .

189   Calcium isotope ratios of calcites and $CaCl_2 \cdot 2H_2O$ used for the growth solutions were

190   measured with a Thermo Fisher Triton TI (Thermal Ionization Mass Spectrometer, TIMS)

191   closely following the procedure described in Heuser et al. (2002). About 2 mg of calcite taken

192   from well-mixed samples or 2 mg of $CaCl_2 \cdot 2H_2O$ were dissolved in 2.2 N ultrapure HCl,

193   evaporated and re-dissolved with a Ca concentration of 160 ng/µL. The solutions were mixed

8

194   with a $^{43}Ca/^{48}Ca$ double spike and evaporated to dryness. About 300 ng of the sample-spike

195   mixture were loaded with 1.5 µl of 2.2 N HCl and 1 µl of $TaCl_5$ activator solution on a zone-

196   refined Re filament for TIMS measurements. More details about the Ca isotope measurements

197   were given in Tang et al. (2008b).

198   Following the suggestion of Eisenhauer et al. (2004), the $^{44}Ca/^{40}Ca$ ratios are reported as

199     $\delta^{44/40}Ca$ (‰) values relative to the NIST standard SRM915a, where $\delta^{44/40}Ca$ =

200     $[(^{44}Ca/^{40}Ca)_{sample}/(^{44}Ca/^{40}Ca)_{SRM915a}$ - 1]×1000. Calcium isotope fractionation between calcite

201   and solution is expressed as $\Delta^{44/40}Ca_{calcite-aq} = \delta^{44/40}Ca_{calcite} - \delta^{44/40}Ca_{aq}$, where $\delta^{44/40}Ca_{calcite}$

202   and $\delta^{44/40}Ca_{aq}$ are the Ca isotope composition of calcite and the growth solution, respectively.

203   The $\delta^{44/40}Ca$ of $CaCl_2 \cdot 2H_2O$ was determined as 1.10±0.04 ‰ (±2 standard errors of the mean,

204   n=9) in the first set of experiments (#1-22, Table 1) and 0.98±0.08 ‰ (n=5) in experiments # 23-

205   26. The external reproducibility of $\delta^{44/40}Ca$, based on repeated measurements of NIST SRM

206   915a, was ±0.10 ‰ (standard deviation, n=52). IAPSO seawater standards measured during

207   sample analyses showed a $\delta^{44/40}Ca$ of 1.84±0.08 ‰ (±2 standard errors of the mean, n=13). Total

208   Ca blanks for the isotope analyses were less than 1%.

209

210   **3. RESULTS**

211   Calculated ionic strengths/salinities, estimated precipitation rates, and measured D_{Sr} and

212     $\Delta^{44/40}Ca_{calcite-aq}$ values for each experiment are given in Table 1.

213

214   **3.1 D_{Sr} values measured at different ionic strengths/salinities**

215   D_{Sr} values measured at different ionic strengths are plotted in Fig. 2 as a function of

216   precipitation rate (R). As shown in Fig. 2, Sr incorporation into calcite is highly influenced by

217   precipitation rate. D_{Sr} values generally increase with increasing precipitation rates. By contrast,

218   an increase of ionic strength from 35 mM to 832 mM (salinity from ~2‰ to 49‰) only leads to

219   some variations in D_{Sr} values. It is not very clear that D_{Sr} values will decrease with increasing

220   ionic strengths, mainly due to the scattered data points obtained at an ionic strength of 292 mM

221   (see Fig. 2).

222   To identify the contribution of precipitation rate (R) and ionic strength (I) to variation in

223   D_{Sr} values, linear regression analyses were carried out using the statistic software R (version

224   2.7.1). Table 2 presents linear regression results in detail. According to linear regression analyses,

225   the relationship between log D_{Sr} and log R at three ionic strengths investigated in this study can

226   be described as follows,

227     $$\log D_{Sr} = (-1.571 \pm 0.171) + (0.176 \pm 0.053) \cdot \log R \tag{3}$$

228     $\{r^2 = 0.667, p = 3.60 \times 10^{-7}, n = 26\}$

229   Equation (3) is very similar to the rate equation of D_{Sr} at 25ºC and ionic strength = 35 mM

230   reported in our previous study (Tang et al., 2008a). But r^2 value for Eqn. (3) is 0.667, whereas r^2

231   value for the rate equation of D_{Sr} at 25ºC and ionic strength = 35 mM is 0.97 (Tang et al., 2008a).

232   This indicates that variation in ionic strength weakens the relationship between log D_{Sr} and log R

233   at 25ºC. The contribution of both precipitation rate (R) and ionic strength (I) to variation in D_{Sr}

234   values can be described as follows,

235     $$\log D_{Sr} = (-1.566 \pm 0.136) + (0.186 \pm 0.043) \cdot \log R - (0.170 \pm 0.091) \cdot I \tag{4}$$

236     $\{r^2 = 0.798, p = 1.03 \times 10^{-8}, n = 26\}$

237   Equation (4) indicates that increase of ionic strength statistically decreases D_{Sr} values.

238   In Table 2, "p-value" for each variable (i.e., log R or I) is the possibility that the

239   coefficient (slope) of each variable = 0, in other words, the possibility that there is no

240   relationship between log D_{Sr} and log R or I. The "p-value" for the regression equation is the

241   possibility that all coefficients (slopes) are 0, in other words, the possibility that this regression

242   equation is caused by the noisy data. In the test of significance, typical values for the significance

243   level are 0.1, 0.05, and 0.01. In this study, we choose 0.01 as the significance level. If "p-value"

244   is less than or equal to 0.01, the influence of precipitation rate (R) or ionic strength (I) to D_{Sr}

245   values is considered to be statistically significant. As shown in Table 2, "p-values" for the slope

246   of log R = 0 are far less than 0.01 in both single and multiple linear regressions. Therefore,

247   precipitation rate (R) surely influences observed D_{Sr} values. The "p-value" for the slope of ionic

248   strength (I) = 0 in a multiple linear regression is 7.97e-4, less than 0.01. Thus, it is valid to say

249   that ionic strength (I) also influences observed D_{Sr} values.

250   Although "p-values" indicate that both precipitation rate (R) and ionic strength (I) will

251   influence Sr partitioning, r^2 (the square of the correlation) values in Table 2 tell us that Sr

252   partitioning is mainly controlled by precipitation rate (R). As shown in Table 2, "r^2" for a simple

253   linear regression between log D_{Sr} and log R is 0.667, which means that 66.7% of variation in log

254   D_{Sr} values is caused by log R. Value of "r^2" for a multiple linear regression between log D_{Sr} and

255   log R + ionic strength (I) is 0.798, which means that the additional effect of ionic strength (I)

256   only accounts for 13.1% (i.e., 0.798-0.667) of variation in log D_{Sr} values.

257   Previous studies (e.g., Zhang and Dawe, 1998; Zuddas and Mucci, 1998) indicate that an

258   increase of ionic strength might increase precipitation rate. To evaluate the possible effect of

259   ionic strength on precipitation rate in our experiments, an ideal way is to conduct the

260   experiments at the same conditions except for ionic strength and to determine precipitation rates

261   at different ionic strengths. Unfortunately, we did not conduct such a series of experiments.

262   However, statistical analyses might provide useful information to test the correlation between

263   precipitation rate and ionic strength in our experiments. In multiple linear regressions, if there is

264   a correlation between two variables, one of them should be eliminated from the regression model.

265   When a variable was eliminated from the regression model, calculated AIC (Akaike's

266   Information Criterion) value for the model will change. The model with the smallest AIC value

267   is the suitable model. Therefore, calculated AIC values for different linear regression models can

268   provide useful information about any possible correlation between two variables. If an increase

269   in ionic strength leads to an increase in precipitation rate (i.e., there is a correlation between ionic

270   strength and precipitation rate), the elimination of log R or ionic strength (I) from multiple linear

271   regressions would result in a smaller AIC value. Our calculations using the statistic software R

272   (version 2.7.1) show that AIC = -100.33 when log R was eliminated from the linear regression

273   model, AIC = -127.58 when ionic strength (I) was eliminated from the linear regression model,

274   and AIC = -138.56 when both log R and I were included in the linear regression model.

275   Calculated AIC values indicate that elimination of log R or ionic strength (I) did not result in a

276   smaller AIC value and the suitable regression model should include both precipitation rate and

277   ionic strength. This means that there is no significant correlation between precipitation rate and

278   ionic strength.

279   In summary, our linear regression analyses indicate that ionic strength indeed influences

280   Sr partitioning, supported by "p-values" for the slope of ionic strength (I) = 0 in a multiple linear

281   regression and calculated AIC values. However, calculated "r^2" values indicate that ionic

282   strength influences Sr partitioning in a minor degree and Sr partitioning is mainly controlled by

283   precipitation rate. Calculated AIC values also indicate that precipitation rates are not

284   significantly affected by ionic strength in our inorganic calcite formation experiments.

285

286   **3.2 $\Delta^{44/40}Ca_{calcite-aq}$ values measured at different ionic strengths/salinities**

287   When $\Delta^{44/40}Ca_{calcite-aq}$ values measured at different ionic strengths are plotted as a

288   function of precipitation rate (Fig. 3), it is obvious that precipitation rate is the primary factor

289   that controls Ca isotope fractionation between precipitated calcite and the growth solution. In

290   general, a fast precipitation will result in a larger absolute $\Delta^{44/40}Ca_{calcite-aq}$ value. The presence of

291   NaCl in the growth solution leads to some variations in $\Delta^{44/40}Ca_{calcite-aq}$ values. But Fig. 3 shows

292   that $\Delta^{44/40}Ca_{calcite-aq}$ values are less sensitive to changes in ionic strengths than to changes in

293   precipitation rates.

294   Linear regression analyses were also carried out using the statistic software R (version

295   2.7.1) to evaluate the contribution of precipitation rate (R) and ionic strength (I) to variation in

296      $\Delta^{44/40}Ca_{calcite-aq}$ values. Table 3 presents linear regression results in detail. Linear regression

297   results show that the relationship between $\Delta^{44/40}Ca_{calcite-aq}$ and log R at three ionic strengths

298   investigated in this study can be described as follows,

299      $\Delta^{44/40}Ca_{calcite-aq} = (0.166 \pm 0.408) - (0.341 \pm 0.125) \cdot \log R$ (5)

300      $\{r^2 = 0.569, p = 8.48 \times 10^{-6}, n = 26\}$

301   Equation (5) is slightly different to the rate equation of $\Delta^{44/40}Ca_{calcite-aq}$ at 25ºC and ionic strength

302   = 35 mM reported in our previous study (Tang et al., 2008b). This indicates that variation in

303   ionic strength influences the relationship between $\Delta^{44/40}Ca_{calcite-aq}$ and log R at 25ºC in some

304   degree. The contribution of both precipitation rate (R) and ionic strength (I) to variation in

305      $\Delta^{44/40}Ca_{calcite-aq}$ values can be described as follows,

306     $\Delta^{44/40}Ca_{calcite-aq} = (0.157 \pm 0.360) - (0.366 \pm 0.112) \cdot \log R + (0.329 \pm 0.241) \cdot I$ (6)

307     $\{r^2 = 0.68, p = 2.02 \times 10^{-6}, n = 26\}$

308   Equation (6) indicates that increase of ionic strength statistically increases $\Delta^{44/40}Ca_{calcite-aq}$ values.

309   In Table 3, "p-value" and "r^2" have the same definition as those in Table 2. As shown in

310   Table 3, "p-values" for the slope of $\log R = 0$ are far less than 0.01 in both single and multiple

311   linear regressions. Therefore, precipitation rate (R) apparently influences observed $\Delta^{44/40}Ca_{calcite-}$

312     $_{aq}$ values. The "p-value" for the slope of ionic strength (I) = 0 in a multiple linear regression is

313   9.6e-3, slightly less than 0.01. Thus, it is valid to say that ionic strength (I) also influences

314   observed $\Delta^{44/40}Ca_{calcite-aq}$ values.

315   However, r^2 values in Table 3 indicate that Ca isotope fractionation is mainly controlled

316   by precipitation rate (R). As shown in Table 3, "r^2" for a simple linear regression between

317     $\Delta^{44/40}Ca_{calcite-aq}$ and $\log R$ is 0.569, which means that 56.9% of variation in $\Delta^{44/40}Ca_{calcite-aq}$ values

318   are caused by $\log R$. Value of "r^2" for a multiple linear regression between $\Delta^{44/40}Ca_{calcite-aq}$ and

319     $\log R$ + ionic strength (I) is 0.680, which means that the additional effect of ionic strength (I)

320   only accounts for 11.1% (i.e., 0.680-0.569) of variation in $\Delta^{44/40}Ca_{calcite-aq}$ values.

321   Once again, calculated AIC values for linear regressions between $\Delta^{44/40}Ca_{calcite-aq}$ and $\log$

322   R + ionic strength (I) indicate that, in our calcite precipitation experiments, precipitation rate of

323   calcite was not effectively influenced by ionic strength. As discussed above, if there is a

324   correlation between ionic strength and precipitation rate, the elimination of $\log R$ or ionic

325   strength (I) from multiple linear regressions would result in a smaller AIC value. Our

326   calculations using the statistic software R (version 2.7.1) show that, in linear regressions between

327     $\Delta^{44/40}Ca_{calcite-aq}$ and $\log R$ + ionic strength (I), AIC = -61.48 when $\log R$ was eliminated from the

328   linear regression model, AIC = -82.24 when ionic strength (I) was eliminated from the linear

14

329 regression model, and AIC = -87.99 when both log R and I were included in the linear regression

330 model. Calculated AIC values show that elimination of log R or ionic strength (I) did not result

331 in a smaller AIC value and the suitable regression model should include both precipitation rate

332 and ionic strength.

333   In summary, linear regression analyses indicate that ionic strength plays a similar role in

334 Ca isotope fractionation as it does in Sr partitioning. That is, ionic strength indeed influences Ca

335 isotope fractionation, supported by "p-values" for the slope of ionic strength (I) = 0 in a multiple

336 linear regression (see Table 3) and calculated AIC values. However, calculated "r^2" values (see

337 Table 3) indicate that ionic strength influences Ca isotope fractionation in a minor degree and Ca

338 isotope fractionation is mainly controlled by precipitation rate.

339

340 **3.3 Relationship between D_{Sr} and $\Delta^{44/40}Ca_{calcite-aq}$ at different ionic strengths/salinities**

341   In our previous study (Tang et al., 2008b), we noticed a strong relationship between D_{Sr}

342 and $\Delta^{44/40}Ca_{calcite-aq}$ and this relationship was observed to be independent of temperature,

343 precipitation rate, and Sr/Ca ratio in the growth solution. Our new experimental data further

344 verify this relationship and document that the strong relationship between D_{Sr} and $\Delta^{44/40}Ca_{calcite-aq}$

345 is also independent of ionic strength from about 35 up to 832 mM (Fig. 4).

346

347 **4. DISCUSSION**

348 **4.1 Salinity/Ionic strength effect on Sr^{2+}/Ca^{2+} in calcite**

349   In our experiments, calcite spontaneously grew from solution. Under such conditions, the

350 increase of ionic strength from about 35 to 832 mM has no significant influence on D_{Sr} values at

351 constant apparent precipitation rates (see Fig. 2). Statistical analysis (see above) reveals that

352   observed variation in D_{Sr} values is largely driven by precipitation rate in accordance with our

353   earlier results (Tang et al., 2008a). Ionic strength effects are minor and only contribute to 13.1%

354   of the explained variation in D_{Sr} values. Because, in the multiple linear regression, the "p-value"

355   for the slope of ionic strength =0 is less than 0.01, a correlation between ionic strength and D_{Sr}

356   values does exist, although the contribution of ionic strength to variation in D_{Sr} values is minor.

357   In accordance with this result, previous studies (e.g., Holland et al., 1963, 1964; Gaetani and

358   Cohen, 2006) reported an insignificant ionic strength effect on D_{Sr} values (also called partition

359   coefficient, k_{Sr}, within some studies) in unseeded experiments, where inorganic calcium

360   carbonate was spontaneously precipitated. However, a strong ionic strength effect on Sr

361   distribution coefficient of calcite was observed in experiments of Pingitore and Eastman (1986),

362   where seeds were used to induce calcite precipitation. In their experiments, elevated ionic

363   strength depressed Sr incorporation into calcite (causing low D_{Sr} values). Besides ionic strength

364   effect, Pingitore and Eastman (1986) also reported a strong effect of aqueous Sr concentration on

365   D_{Sr} values. In contrast, in experiments where inorganic calcium carbonates were spontaneously

366   precipitated (Holland et al., 1963, 1964; Gaetani and Cohen, 2006; Tang et al., 2008a), D_{Sr}

367   values were independent of Sr concentrations in the growth solution. Thus, different

368   experimental conditions might result in distinct Sr incorporation behavior into calcite.

369   Pingitore and Eastman (1986) used a multiple site model to interpret the effects of

370   aqueous Sr concentration and ionic strength and on their k_{Sr} values (given as D_{Sr} in the following

371   text). More specifically, Pingitore and Eastman (1986) argued that two types of sites are involved

372   in Sr incorporation during calcite formation: (1) normal lattice sites and (2) non-lattice sites

373   (wherein site defects favor Sr versus Ca incorporation). The abundance of non-lattice sites is less

374   than that of normal lattice sites. As a result, non-lattice contribution to D_{Sr} is significant at low

16

375 aqueous Sr concentrations and becomes less important with increasing aqueous Sr concentrations.

376 Thus, measured D_{Sr} values depend inversely on aqueous Sr concentrations in their experiments.

377 Using the multiple site model, Pingitore and Eastman (1986) interpreted that the decrease in D_{Sr}

378 values with increasing ionic strength was owing to competition between Sr^{2+} and Na^+ ions for

379 non-lattice sites. If both normal lattice sites and non-lattice sites were involved in Sr

380 incorporation and Na competes for limited non-lattice sites with Sr, higher Na concentration at

381 high ionic strength will lower Sr incorporation at constant R. Thus, the multiple site model of

382 Pingitore and Eastman (1986) might be reasonable to describe Sr incorporation into calcite under

383 their experimental conditions where seeds were used to induce calcite precipitation.

384   But from the view of kinetics of calcite growth, strong negative ionic strength effect on

385 D_{Sr} values observed by Pingitore and Eastman (1986) is perplexing. Previous studies on the

386 influence of high ionic strength on inorganic calcite precipitation using a seed-induced technique

387 (e.g., Zhang and Dawe, 1998; Zuddas and Mucci, 1998) suggest that the precipitation rate of

388 calcite will increase with increasing ionic strength. It is well documented that Sr incorporation

389 into calcite is a precipitation rate-controlled process and fast precipitation leads to a larger D_{Sr}

390 value (Fig. 2; Lorens, 1981; Tesoriero and Pankow, 1996; Tang et al., 2008a). Thus, during seed-

391 induced precipitations, D_{Sr} values are expected to be positively correlated with ionic strength,

392 because an increase in ionic strength will result in an increase in precipitation rate and thus an

393 increase in D_{Sr} values. Indeed, several culture experiments (i.e., Lea et al., 1999; Kısakürek et al.,

394 2008; Dissard et al., 2010) reported that Sr/Ca ratio in foraminiferal calcite increases with

395 increasing salinity. Because all these culture experiments suggest that the Sr/Ca ratios in

396 foraminiferal calcite are primarily controlled by the growth rate, the positive relationship

397 between salinity and Sr/Ca ratios observed in these culture experiments was unanimously

17

398 interpreted by the corresponding authors as a result of a kinetic effect, i.e., salinity indirectly

399 influences the Sr/Ca ratios most likely through its impact on the growth rate of foraminiferal

400 calcite. In a word, a strong negative correlation between ionic strength and Sr partitioning

401 observed in Pingitore and Eastman (1986)'s seed-induced calcite precipitations is inconsistent

402 with a weakly positive correlation between ionic strength and Sr partitioning reported in most of

403 previous studies and is difficult to understand in view of kinetics of calcite growth.

404   In current studies as well as previous experiments where inorganic calcium carbonates

405 were spontaneously precipitated (Holland et al., 1963, 1964; Gaetani and Cohen, 2006; Tang et

406 al., 2008a), D_{Sr} values were independent of Sr concentrations in the growth solution and weakly

407 influenced by ionic strength. This is inconsistent with the significant non-lattice contribution to

408 D_{Sr} at low aqueous Sr concentrations and the competition for non-lattice sites between Na^+ and

409 Sr^{2+} at high ionic strengths suggested by the multiple site model. Thus, the multiple site model is

410 not applicable to spontaneous calcite precipitation. Moreover, linear regression analyses (see

411 Sections 3.1 and 3.2) indicate that, in our spontaneous calcite precipitations, ionic strength is not

412 correlated with precipitation rate, at least not at a statistic significance level. This is inconsistent

413 with a positive correlation between ionic strength and precipitation rate observed in seed-induced

414 calcite preccipitation (e.g., Zhang and Dawe, 1998; Zuddas and Mucci, 1998). Therefore, we

415 argue that main controls on calcite growth are different between seed-induced precipitation and

416 spontaneous precipitation. Calcite growth rates are not only controlled by the degree of

417 supersaturation but also affected by aqueous Ca^{2+}/CO_3^{2-} ratio (Nehrke et al., 2007), ionic strength

418 (Zhang and Dawe, 1998; Zuddas and Mucci, 1998), and pH (Ruiz-Agudo et al., 2011). The

419 degree of supersaturation is relatively lower during seed-induced precipitation than during

420 spontaneous precipitation. As a result, the solution composition such as aqueous Ca^{2+}/CO_3^{2-} ratio,

421 ionic strength, and pH might play a larger role in calcite growth during seed-induced

422 precipitation, whereas, the degree of supersaturation might play a more important role in calcite

423 growth during spontaneous precipitation. In addition, during seed-induced precipitation, Sr

424 partitioning may occur at the surface of seeds and the multi sites may already exist for the

425 competition between Na^+ and Sr^{2+}. But during spontaneous precipitation, there are no existing

426 surface sites and Sr partitioning might be mainly controlled by the first nucleus of crystal at

427 critical supersaturation. Therefore, during spontaneous precipitation such as our inorganic calcite

428 formation, Sr partitioning is mainly controlled by precipitation rate and ionic strength only plays

429 a minor role in Sr partitioning.

430   According to our previous studies (Tang et al., 2008a), Sr partitioning in calcite under our

431 experimental conditions can be successfully interpreted by the surface enrichment model

432 (SEMO), i.e., the degree of disequilibrium Sr partitioning in calcite depends on the competition

433 between the entrapment of the composition of Sr-enriched surface layer by crystal growth and

434 the ion diffusion in the newly formed crystal lattice. Fast precipitation will favor the entrapment

435 of the composition of Sr-enriched surface layer and increase the distance for ion diffusion in the

436 newly formed crystal lattice. As a result, Sr partitioning is sensitive to precipitation rate.

437 However, ionic strength does not effectively influence calcite growth in our experiments

438 suggested by linear regression analyses (see Section 3.1) and cannot influence ion diffusion as

439 temperature does. Therefore, a weak impact of ionic strength on Sr partitioning is expected by

440 the surface entrapment model.

441

442 **4.2 Salinity/Ionic strength effect on $^{44}Ca/^{40}Ca$ ratios in calcite**

443   An increase of ionic strength from 35 mM to 832 mM (salinity from ~2‰ to 49‰) does

444   not significantly change the $\Delta^{44/40}Ca_{calcite-aq}$ values in our experiments at a given precipitation rate

445   (see Table 1). Instead, $\Delta^{44/40}Ca_{calcite-aq}$ values of calcite precipitated at different ionic strengths

446   generally follow the same trend in the plot of $\Delta^{44/40}Ca_{calcite-aq}$ versus log R (see Fig. 3). Statistical

447   analysis (see above) indicates that ionic strength effects only account for 11.1% of the explained

448   variation in $\Delta^{44/40}Ca_{calcite-aq}$ values. However, in the multiple linear regression between

449    $\Delta^{44/40}Ca_{calcite-aq}$ and log R + ionic strength (I), the p value for the slope of ionic strength = 0 is

450   close to 0.01 but less than 0.05. Thus, it is still valid to say that ionic strength indeed influences

451    $\Delta^{44/40}Ca_{calcite-aq}$ values during inorganic calcite formation. Our results suggest that precipitation

452   rate is the primary factor that controls Ca isotope fractionation during inorganic calcite formation

453   at 25°C. To our knowledge, few studies have been carried out to investigate systematically ionic

454   strength effect on Ca isotopes in calcium carbonates. Lemarchand et al. (2004) precipitated

455   inorganic calcite spontaneously from two types of growth solutions with ionic strength of 450

456   and 850 mM, respectively (salinity of 22.7 and 37.8‰, respectively). In their $\Delta^{44/40}Ca$ vs log R

457   plot no difference between the two solutions was obtained (see Fig.7 in Lemarchand et al., 2004).

458   In accordance, culture experiments with the dinoflagellate species *Thoracosphaera heimii* by

459   Gussone et al. (2010) indicate that there is no significant correlation between the analyzed

460    $^{44}Ca/^{40}Ca$ ratio in $CaCO_3$ and salinity. On the other hand, culturing experiments on planktic

461   foraminifera, *Globigerinoides ruber* and *Globigerinella siphonifera*, by Kısakürek et al. (2011)

462   demonstrated systematic variations in $\delta^{44/40}Ca$ with salinity. Although the total variation in the

463   studied species was on the same order as the external reproducibility, the salinity response of

464   calcium isotope ratios was consistent with a kinetic effect. Therefore, studies on inorganic calcite

465   and coccolithophores suggest that $^{44}Ca/^{40}Ca$ ratios in calcite are weakly influenced by ionic

466   strength, whereas in low Mg foraminifera, ionic strength appears to have a noticeable effect on

467   calcium isotope fractionation through kinetics of calcite growth.

468   According to our previous studies (Tang et al., 2008b), Ca isotope fractionation during

469   inorganic calcite formation under our experimental conditions can also be successfully

470   interpreted by the surface enrichment model (SEMO). Based on SEMO model calculations (see

471   Tang et al., 2008b for the calculations in detail), precipitation rate effect on Ca isotope

472   fractionation is due to the effective entrapment of ^{44}Ca-depleted surface layer by crystal growth

473   before ion diffusion re-equilibrates any abnormal composition in the newly-formed crystal lattice.

474   Although ionic strength does not effectively influence calcite growth in our experiments

475   suggested by linear regression analyses (see section 3.2) and cannot influence ion diffusion as

476   temperature does, ionic strength might influence the composition of the surface layer as we

477   discussed in Tang et al. (2008b). Therefore, a weak impact of ionic strength on Ca isotope

478   fractionation is expected by the surface entrapment model.

479

480   **4.3 Sr/Ca and ^{44}Ca/^{40}Ca ratios in calcite as environmental proxies**

481   In our previous studies (Tang et al., 2008a, b), we discussed the potential use of Sr/Ca

482   and ^{44}Ca/^{40}Ca ratios in calcite as environmental proxies based on our experiments. Our previous

483   experiments demonstrated that both Sr/Ca and ^{44}Ca/^{40}Ca ratios in calcite are sensitive to

484   precipitation rate and temperature. Neither precipitation rate nor temperature dominantly

485   controlled Sr/Ca and ^{44}Ca/^{40}Ca ratios. Thus, we argued that Sr/Ca and ^{44}Ca/^{40}Ca ratios could be

486   used as an indicator of precipitation rate or temperature if one of these two factors was well-

487   known. However, at that time, because all of our experiments were conducted at low ionic

488   strength/salinity, we pointed out that the application of Sr/Ca and ^{44}Ca/^{40}Ca ratios as

489 environmental proxies was only valid in terrestrial water systems and might be limited in marine

490 environments. Our new experimental data presented in this study provide strong evidence that

491 both Sr/Ca and $^{44}Ca/^{40}Ca$ ratios in calcite are weakly influenced by ionic strength/salinity. Thus,

492 Sr/Ca and $^{44}Ca/^{40}Ca$ ratios can also be used individually as an environmental proxy or be

493 combined as a multi-proxy application in paleoceanographic studies. As both Sr/Ca and

494 $^{44}Ca/^{40}Ca$ ratios are sensitive to temperature (see Tang et al., 2008a, b) but weakly influenced by

495 ionic strength (see Figs. 2, 3), Sr/Ca and $^{44}Ca/^{40}Ca$ ratios in marine calcites not only provide

496 information about SST, but also are helpful to isolate salinity effects from temperature effects in

497 stable oxygen isotope signals.

498 The strong relationship between $\log D_{Sr}$ and $\Delta^{44/40}Ca_{calcite-aq}$, independent of

499 environmental factors (e.g., temperature, aqueous Sr/Ca ratio, precipitation rate, salinity/ionic

500 strength; Fig. 4; see also Tang et al., 2008b), reflects the same mechanism (i.e., the surface

501 entrapment by crystal growth) controlling both Sr incorporation and Ca isotope fractionation

502 during inorganic calcite formation (Tang et al., 2008b). This strong relationship between $\log D_{Sr}$

503 and $\Delta^{44/40}Ca_{calcite-aq}$ can be found in both biogenic and inorganic calcite (see Fig. 7 of Tang et al.,

504 2008b) and thus can be used to recalculate Sr/Ca or Ca isotopic composition in calcite if

505 reasonable assumptions of the aqueous Sr/Ca ratio or Ca isotopic composition can be made. For

506 this purpose, knowledge on environmental parameters during calcite formation like temperature,

507 precipitation rate, and ionic strength is not required (see Fig.4). Moreover, any deviation from

508 the $\log D_{Sr} / \Delta^{44/40}Ca_{calcite-aq}$ relationship can be used to decipher the diagenetic $CaCO_3$ alteration.

509

510 **5. CONCLUSION**

511   Our experiments indicate that Sr/Ca and $^{44}Ca/^{40}Ca$ ratios in calcite are primarily

512   controlled by precipitation rate at 25ºC. The rate-dependence of Sr/Ca and $^{44}Ca/^{40}Ca$ ratios in

513   calcite is not sensitive to variations in ionic strength investigated in our experiments. Thus, ionic

514   strength has a weak impact on Sr/Ca and $^{44}Ca/^{40}Ca$ ratios in calcite. The positive linear

515   relationship between salinity and Sr/Ca ratio observed in biogenic calcite can be reasonably

516   explained by more rapid kinetics of calcite growth caused by the increase of salinity.

517   A strong correlation between the Sr distribution coefficient and $^{44}Ca/^{40}Ca$ isotope

518   fractionation of calcite is not affected by changes in ionic strength, which verifies that the surface

519   entrapment mechanism may control both Sr incorporation and Ca isotope fractionation during

520   calcite formation as pointed out in our previous study (Tang et al., 2008b). Our experiments

521   show a weak impact of ionic strength on both Sr/Ca and $^{44}Ca/^{40}Ca$ ratios in calcite. Thus, if the

522   rates of calcite growth can be approximated, Sr/Ca and $^{44}Ca/^{40}Ca$ ratios in marine calcium

523   carbonates may be used as proxies for SST, but also to discriminate between temperature and

524   salinity effects on oxygen isotope ratios in marine calcium carbonates. The strong correlation

525   between Sr partitioning and Ca isotope fractionation in calcite can be used to reveal the solid

526   composition of calcite, i.e., $^{44}Ca/^{40}Ca$ ratio in calcite can be estimated from Sr/Ca ratio and vice

527   versa, if reasonable assumptions of the aqueous Sr/Ca ratio or Ca isotopic composition can be

528   made. What is more, the estimation of $^{44}Ca/^{40}Ca$ ratio or Sr/Ca ratio can be made even when

529   environmental parameters during calcite formation such as temperature, precipitation rate, and

530   ionic strength are unknown.

538   **References**

539   Arbuszewski J., deMenocal P., Kaplan A., and Farmer E. C. (2010) On the fidelity of shell-

540   derived $\delta^{18}O_{seawater}$ estimates. *Earth Planet. Sci. Lett.* **300**, 185-196.

541   Barker S., Cacho I., Benway H., and Tachikawa K. (2005) Planktonic foraminiferal Mg/Ca as a

542   proxy for past oceanic temperatures: a methodological overview and data compilation for

543   the last glacial maximum. *Quat. Sci. Rev.* **24**, 821-834.

544   Corrège T. (2006) Sea surface temperature and salinity reconstruction from coral geochemical

545   tracers. *Paleogeogr. Paleoclimatol. Paleoecol.* **232**, 408-428.

546   Dietzel M., Gussone N., and Eisenhauer A. (2004) Co-precipitation of Sr^{2+} and Ba^{2+} with

547   aragonite by membrane diffusion of CO_2 between 10 and 50ºC. *Chem. Geol.* **203**, 139-

548   151.

549   Dissard D., Nehrke G., Reichart G. J., Bijma J. (2010) The impact of salinity on the Mg/Ca and

550   Sr/Ca ratio in the benthic foraminifera Ammonia tepida: Results from culture

551   experiments. *Geochim. Cosmochim. Acta* **74**, 928-940.

552   Dueñas-Bohórquez A., da Rocha R. E., Kuroyanagi A., Bijma J., Reichart G.-J. (2009) Effect of

553   salinity and seawater calcite saturation state on Mg and Sr incorporation in cultured

554   planktonic foraminifera. *Mar. Micropaleontol.* **73**, 178-189.

555   Eisenhauer A., Nägler T., Stille P., Kramers J., Gussone N., Bock B., Fietzke J., Hippler D., and

556   Schmitt A.-D. (2004) Proposal for an international agreement on Ca notation as result of

557   the discussions from the workshops on stable isotope measurements in Davos

558   (Goldschmidt 2002) and Nice (EGS-AGU-EUG 2003). *Geostand.Geoanal. Res.* **28,** 149–

559   151.

25

560   Eisma D., Mook W. G., and Das H. A. (1976) Shell characteristics, isotopic composition and

561   trace-element contents of some euryhaline molluscs as indicators of salinity. *Paleogeogr.*

562   *Paleoclimatol. Paleoecol.* **19**, 39-62.

563   Elderfield H. and Ganssen G. (2000) Past temperature and $\delta^{18}O$ of surface ocean waters inferred

564   from foraminiferal Mg/Ca ratios. *Nature* **405**, 442-445.

565   Ferguson J.E., Henderson G.M., Kucera M., Rickaby R.E.M. (2008) Systematic change of

566   foraminiferal Mg/Ca ratios across a strong salinity gradient. *Earth Planet. Sci. Lett.* **265**,

567   153-166.

568   Gaetani, G.A. and Cohen, A.L. (2006) Element partitioning during precipitation of aragonite

569   from seawater: A framework for understanding paleoproxies. *Geochim. Cosmochim. Acta*

570   **70**, 4617-4634.

571   Gussone N., Eisenhauer A., Tiedemann R., Haug G.H., Heuser A., Bock B., Nägler Th.F., and

572   Müller A. (2004) Reconstruction of Caribbean Sea surface temperature and salinity

573   fluctuations in response to the Pliocene closure of the Central American Gateway and

574   radiative forcing, using $\delta^{44/40}Ca$, $\delta^{18}O$, and Mg/Ca ratios. *Earth Planet. Sci. Lett.* **227**,

575   201-214.

576   Gussone N., Zonneveld K., and Kuhnert H. (2010) Minor element and Ca isotope composition of

577   calcareous dinoflagellate cysts of cultured *Thoracosphaera heimii*. *Earth Planet. Sci.*

578   *Lett.* **289**, 180-188.

579   Heuser, A., Eisenhauer, Gussone, N., Bock, B., Hansen, B.T., and Nägler, T.F. (2002)

580   Measurement of calcium isotopes ($\delta^{44}Ca$) using a multicollector TIMS technique. *Int. J.*

581   *Mass Spectrom.* **220**, 387-399.

582 Hoogakker B. A.A., Klinkhammer G. P., Elderfield H., Rohling E. J., and Hayward C. (2009)

583   Mg/Ca paleothermometry in high salinity environments. *Earth Planet. Sci. Lett.* **284**,

584   583-589.

585 Holland H. D., Borcsik M., Munoz J., and Oxburgh U. M. (1963) The coprecipitation of Sr^{+2}

586   with aragonite and of Ca^{+2} with strontianite between 90 ° and l00 ºC. *Geochim.*

587   *Cosmochim. Acta* **27**, 957-977.

588 Holland H.D., Holland H.J., and Munoz J.L. (1964) The coprecipitation of cations with $CaCO_3$-

589   II. The coprecipitation of Sr^{+2} with calcite between 90º and 100ºC. *Geochim. Cosmochim.*

590   *Acta* **28**, 1287-1301.

591 Katz A., Sass E., Starinsry A., and Holland H. D. (1972) Strontium behavior in the aragonite-

592   calcite transformation: An experimental study at 40-98ºC. *Geochim. Cosmochim. Acta*

593   **36**, 481-496.

594 Kısakürek B., Eisenhauer A., Böhm F., Garbe-Schönberg D., and Erez J. (2008) Controls on

595   shell Mg/Ca and Sr/Ca in cultured planktonic foraminiferan, *Globigerinoides ruber*

596   (white). *Earth Planet. Sci. Lett.* **273**, 260-269.

597 Kısakürek B., Eisenhauer A., Böhm F., Hathorne E. C.., and Erez J. (2011) Controls on calcium

598   isotope fractionation in cultured planktic foraminifera, *Globigerinoides ruber* and

599   *Globigerinella siphonifera. Geochim. Cosmochim. Acta* **75**, 427-443.Klein R. T.,

600   Lohmann K. C., and Thayer W. (1996) Sr/Ca and $^{13}C/^{12}C$ ratios in skeletal calcite of

601   *Mytilus trossulus*: Covariation with metabolic rate, salinity, and carbon isotopic

602   composition of seawater. *Geochim. Cosmochim. Acta* **60**, 4027-4221.

603   Lea D. W., Mashiotta T. A., and Spero H. J. (1999) Controls on magnesium and strontium

604   uptake in planktonic foraminifera determined by live culturing. *Geochim. Cosmochim.*

605   *Acta* **63**, 2369-2379.

606   Lemarchand, D., Wasserburg, G.J., and Papanastassiou, D.A. (2004) Rate-controlled calcium

607   isotope fractionation in synthetic calcite. *Geochim. Cosmochim. Acta* **68**, 4665-4678.

608   Lorens, R.B. (1981) Sr, Cd, Mn and Co distribution coefficients in calcite as a function of calcite

609   precipitation rate. *Geochim. Cosmochim. Acta* **45**, 553 -561.

610   Mucci A. and Morse J. W. (1983) The incorporation of Mg^{2+} and Sr^{2+} into calcite overgrowth:

611   influence of growth rate and solution composition. *Geochim. Cosmochim. Acta* **47**, 217-

612   233.

613   Nehrke, G., Reichart, G.J., Van Cappellen, P., Meile, C., and Bijma, J. (2007) Dependence of

614   calcite growth rate and Sr partitioning on solution stoichiometry: Non-Kossel crystal

615   growth. *Geochim. Cosmochim. Acta* **71**, 2240-2249.

616   Nürnberg D., Bijma J., and Hemleben C. (1996) Assessing the reliability of magnesium in

617   foraminiferal calcite as a proxy for water mass temperatures. *Geochim. Cosmochim. Acta*

618   **60**, 803-814.

619   Pingitore N. E., Jr., and Eastman M. P. (1986) The coprecipitation of Sr^{2+} with calcite at 25°C

620   and 1 atm. *Geochim. Cosmochim. Acta* **50**, 2195-2203.

621   Rosales I., Robles S., and Quesada S. (2004) Elemental and oxygen isotope composition of early

622   Jurassic belemnites: salinity vs. temperature signals. *J. Sediment. Res.* **74**, 342-354.

623   Rostek F., Ruhland G., Bassinot F.C., Müller P.J., Labeyrle L.D., Lancelot Y., and Bard E.

624   (1993) Reconstructing sea surface temperature and salinity using $\delta^{18}O$ and alkenone

625   records. *Nature* **364**, 319-321.

626   Ruiz-Agudo E., Putnis, C.V., Rodriguez-Navarro, C., and Putnis, A. (2011) Effect of pH on

627   calcite growth at constant $a_{Ca^{2+}}/a_{CO_3^{2-}}$ ratio and supersaturation. *Geochim. Cosmochim.*

628   *Acta* **75**, 284-296.

629   Sampei Y., Matsumoto E., Dettman D. L., Tokuoka T., and Abe O. (2005) Paleosalinity in a

630   brackish lake during the Holocene based on stable oxygen and carbon isotopes of shell

631   carbonate in Nakaumi Lagoon, southwest Japan. *Paleogeogr. Paleoclimatol. Paleoecol.*

632   **224**, 352-366.

633   Tang J., Köhler S.J., Dietzel M. (2008a) Sr^{2+}/Ca^{2+} and $^{44}Ca/^{40}Ca$ fractionation during inorganic

634   calcite formation: I. Sr incorporation. *Geochim. Cosmochim. Acta* **72**, 3718-3732.

635   Tang J., Dietzel M., Böhm F., Köhler S.J., and Eisenhauer A. (2008b) Sr^{2+}/Ca^{2+} and $^{44}Ca/^{40}Ca$

636   fractionation during inorganic calcite formation: II. Ca isotopes. *Geochim. Cosmochim.*

637   *Acta* **72**, 3733-3745.

638   Tesoriero, A.J., and Pankow, J.F. (1996) Solid solution partitioning of Sr^{2+}, Ba^{2+}, and Cd^{2+} to

639   calcite. *Geochim. Cosmochim. Acta* **60**, 1053-1063.

640   Usdowski, H.E. (1975) *Fraktionierung der Spurenelemente bei der Kristallisation*, Springer-

641   Verlag Berlin, Heidelberg, pp104.

642   Zhang Y.P. and Dawe R. (1998) The kinetics of calcite precipitation from a high salinity water.

643   *Appl. Geochem.* **13**, 177-184.

644   Zuddas, P. and Mucci, A. (1998) Kinetics of calcite precipitation from seawater: II. The

645   influence of the ionic strength. *Geochim. Cosmochim. Acta* **62**, 757-766.

646

Table 1 Experimental data for Sr/Ca and $^{44}Ca/^{40}Ca$ fractionation during inorganic calcite formation from solutions with different salinities/ionic strengths at room temperature (25 ± 0.5 ºC).

No	pH	I (mM)	Salinity (‰)	[NH$_4$Cl] (mM)	[NaCl] (mM)	[Ca]$_o$ (mM)	[Sr]$_o$ (μM)	Sr in calcite (mg/kg CaCO$_3$)	SI$_{calcite}$	log R[#1] (μmol/m^2/h)	log D$_{Sr}$[#2]	$\Delta^{44/40}$Ca$_{calcite-aq}$ (‰) ± 2SEM[#3] (n)
1						9.6	96.1	1477	1.21	4.2	-0.79	-1.50 ± 0.19 (6)
2						9.6	94.6	1131	1.11	3.6	-0.91	-1.17 ± 0.10 (2)
3						9.8	96.7	976	1.11	3.1	-0.97	-1.04 ± 0.10 (4)
4						9.7	95.1	830	0.94	3.0	-1.03	-0.80 ± 0.10 (4)
5						10.0	96.5	600	0.66	2.3	-1.18	-0.62 ± 0.16 (6)
6						9.9	96.1	932	0.89	3.3	-0.97	-1.03 ± 0.12 (4)
7		35	1.8		0	9.9	93.1	525	0.65	2.4	-1.21	-0.51 ± 0.10 (2)
8						9.7	92.1	673	0.69	2.4	-1.12	-0.67 ± 0.10 (2)
9						9.9	94.3	1503	1.21	4.2	-0.76	-1.37 ± 0.15 (7)
10						10.0	94.9	1387	1.12	3.9	-0.79	-1.47 ± 0.17 (6)
11						10.3	96.5	1355	1.23	4.0	-0.81	-1.41 ± 0.10 (2)
12						9.8	0.78	9.37	1.07	3.8	-0.90	-0.93 ± 0.10 (6)
13	8.3			5		9.9	0.67	4.20	0.78	2.4	-1.17	-0.73 ± 0.23 (8)
14						9.9	99.2	1168	0.99	3.0	-0.91	-1.16 ± 0.20 (7)
15						9.3	93.3	1099	0.96	2.8	-0.97	-0.99 ± 0.01 (2)
16						9.2	93.3	1210	0.86	2.7	-0.96	-0.83 ± 0.08 (3)
17		292	16.8		257	9.0	90.2	959	1.17	3.4	-1.03	-0.68 ± 0.20 (5)
18						8.2	82.0	838	1.13	3.2	-1.08	-0.66 ± 0.12 (5)
19						9.2	93.1	1200	1.07	3.2	-0.93	-1.02 ± 0.10 (3)
20						9.7	98.9	532	0.88	2.2	-1.26	-0.71 ± 0.11 (4)
21						8.7	90.7	532	0.84	1.9	-1.25	-0.38 ± 0.05 (3)
22						9.3	87.2	921	1.05	3.6	-0.99	-1.12 ± 0.12 (4)
23						9.1	83.0	598	0.63	3.6	-1.11	-0.91 ± 0.05 (2)
24		832	49		799	9.5	92.0	703	0.80	3.7	-1.07	-0.71 ± 0.06 (2)
25						9.2	91.0	762	1.22	3.7	-1.07	-0.83 ± 0.05 (2)
26						9.6	89.0	806	0.83	3.8	-1.01	-0.79 ± 0.22 (4)

pH: pH of growth solution; I: ionic strength; [Ca]$_o$: initial Ca concentration; [Sr]$_o$: initial Sr concentration; SI$_{calcite}$: critical saturation index with respect to calcite; R: precipitation rate of calcite; D$_{Sr}$: distribution coefficient for Sr in calcite; $\Delta^{44/40}$Ca$_{calcite-aq}$ = $\delta^{44/40}$Ca$_{calcite}$ − $\delta^{44/40}$Ca$_{aq}$. Experiments # 1 to 13 are from Tang et al. (2008b). n is the number of repeat measurements.

[#1] Error of measured precipitation rate is log R ± 0.12, estimated from three duplicate experiments (see Tang et al., 2008a).

[#2] Error of measured Sr distribution coefficient is log D$_{Sr}$ ± 0.03, estimated from three duplicate experiments (see Tang et al., 2008a).

[#3] SEM is the standard error of the mean.

656 Table 2. The output of coefficients and the associated summary for: (a) a simple linear regression
657 between log D_{Sr} and log R; and (b) a multiple linear regression between log D_{Sr} and log R + ionic
658 strength (I)
659

(a)	coefficients	Standard error	t stat	p-value	Lower 95%	Upper 95%
intercept	-1.571	0.083	-19.026	5.55e-16	-1.741	-1.400
log R	0.176	0.025	6.934	3.60e-7	0.123	0.228
summary	The regression equation: log D_{Sr} = (-1.571 ± 0.171) + (0.176 ± 0.053) · log R Residual standard error: 0.08288 on 24 degrees of freedom r^2: 0.667, Adjusted r^2: 0.653 F-statistic: 48.08 on 1 and 24 DF, p-value: 3.6e-7					

660

(b)	coefficients	Standard error	t stat	p-value	Lower 95%	Upper 95%
intercept	-1.566	0.066	-23.832	< 2e-16	-1.702	-1.430
log R	0.186	0.020	9.223	3.44e-9	0.146	0.231
I	-0.170	0.044	-3.859	7.97e-4	-0.261	-0.079
summary	The regression equation: log D_{Sr} = (-1.566 ± 0.136) + (0.186 ± 0.043) · log R – (0.170 ± 0.091) · I Residual standard error: 0.06596 on 23 degrees of freedom r^2: 0.798, Adjusted r^2: 0.780 F-statistic: 45.4 on 2 and 23 DF, p-value: 1.033e-8					

661 Table 3. The output of coefficients and the associated summary for: (a) a simple linear regression
662 between $\Delta^{44/40}Ca_{calcite-aq}$ and log R; and (b) a multiple linear regression between $\Delta^{44/40}Ca_{calcite-aq}$
663 and log R + ionic strength (I)

664

(a)	coefficients	Standard error	t stat	p-value	Lower 95%	Upper 95%
intercept	0.166	0.197	0.841	0.409	-0.242	0.573
log R	-0.341	0.061	-5.632	8.48e-6	-0.466	-0.216
summary	The regression equation is $\Delta^{44/40}Ca_{calcite-aq} = (0.166 \pm 0.408) - (0.341 \pm 0.125) \cdot$ log R Residual standard error: 0.1982 on 24 degrees of freedom r^2: 0.569, Adjusted r^2: 0.551 F-statistic: 31.72 on 1 and 24 DF, p-value: 8.481e-6					

665

(b)	coefficients	Standard error	t stat	p-value	Lower 95%	Upper 95%
intercept	0.157	0.174	0.903	0.376	-0.203	0.517
log R	-0.366	0.054	-6.772	6.6e-7	-0.478	-0.254
I	0.329	0.117	2.825	9.6e-3	0.088	0.570
summary	The regression equation $\Delta^{44/40}Ca_{calcite-aq} = (0.157 \pm 0.360) - (0.366 \pm 0.112) \cdot$ log R + $(0.329 \pm 0.241) \cdot$ I Residual standard error: 0.1744 on 23 degrees of freedom r^2: 0.680, Adjusted r^2: 0.652 F-statistic: 24.46 on 2 and 23 DF, p-value: 2.023e-6					

666

667   Fig. 1 Representative scanning electron micrographs (SEM) of calcite grown from solutions with

668   different ionic strengths: (a) I = 35 mM (No.1 in Table 1); (b) I = 292 mM (No. 18); and (c) I =

669   832 mM (No. 26).

670

671

672   Fig. 2 log D_{Sr} versus log R for inorganic calcite grown from solutions with different ionic

673   strengths. D_{Sr} is the Sr distribution coefficient of calcite. R is the precipitation rate of calcite (T =

674   25°C; pH = 8.3).

675

676   Fig. 3 $\Delta^{44/40}Ca_{calcite-aq}$ versus log R for inorganic calcite grown from solutions with different ionic

677   strengths. $\Delta^{44/40}Ca_{calcite-aq}$ = $\delta^{44/40}Ca_{calcite}$ - $\delta^{44/40}Ca_{aq}$, where $\delta^{44/40}Ca_{calcite}$ is $^{44}Ca/^{40}Ca$ ratio

678   measured in calcite relative to the SRM915a standard and $\delta^{44/40}Ca_{aq}$ is $^{44}Ca/^{40}Ca$ ratio measured

679   in the growth solution relative to the SRM915a standard. R is the precipitation rate of calcite (T

680   = 25°C; pH = 8.3).

681

682   Fig. 4 Correlation between $\Delta^{44/40}Ca_{calcite-aq}$ and log D_{Sr} [$\Delta^{44/40}Ca_{calcite-aq}$ = (-1.90±0.23) · log D_{Sr} -

683   2.85±0.22, R^2 = 0.90, $p<10^{-15}$, n = 31] observed in our experiments conducted at ionic strength

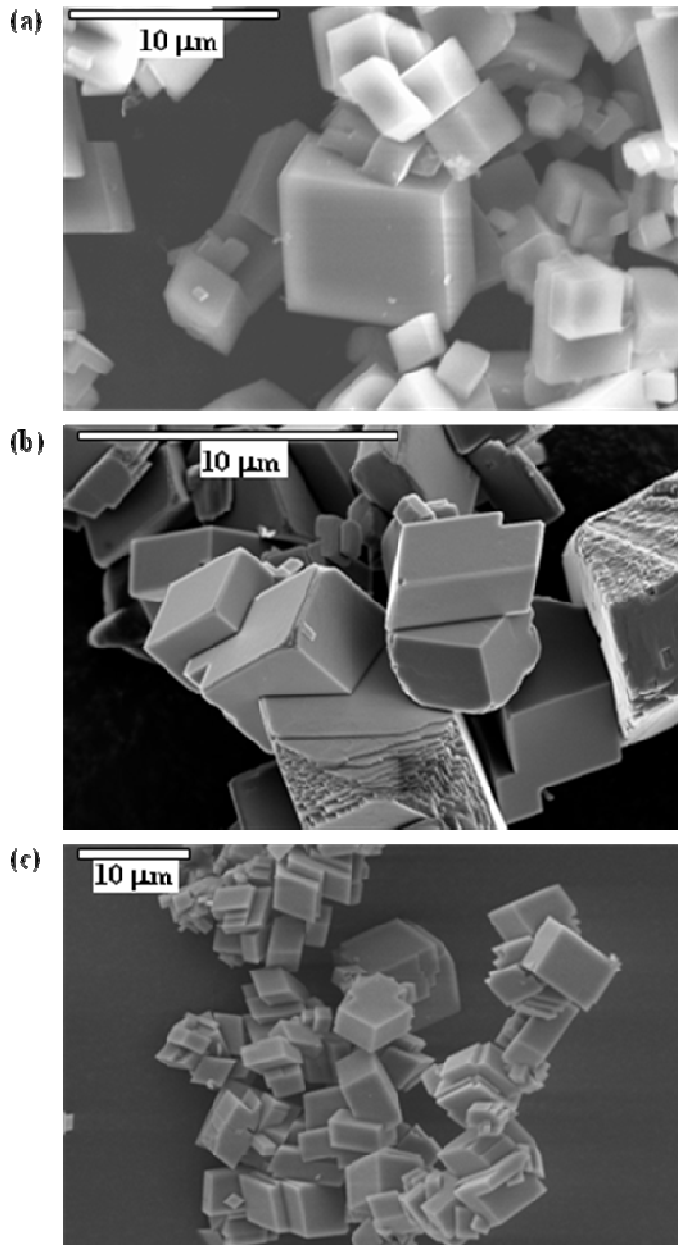684   ranging from 35 to 832 mM (salinity from ~2‰ to 49‰).
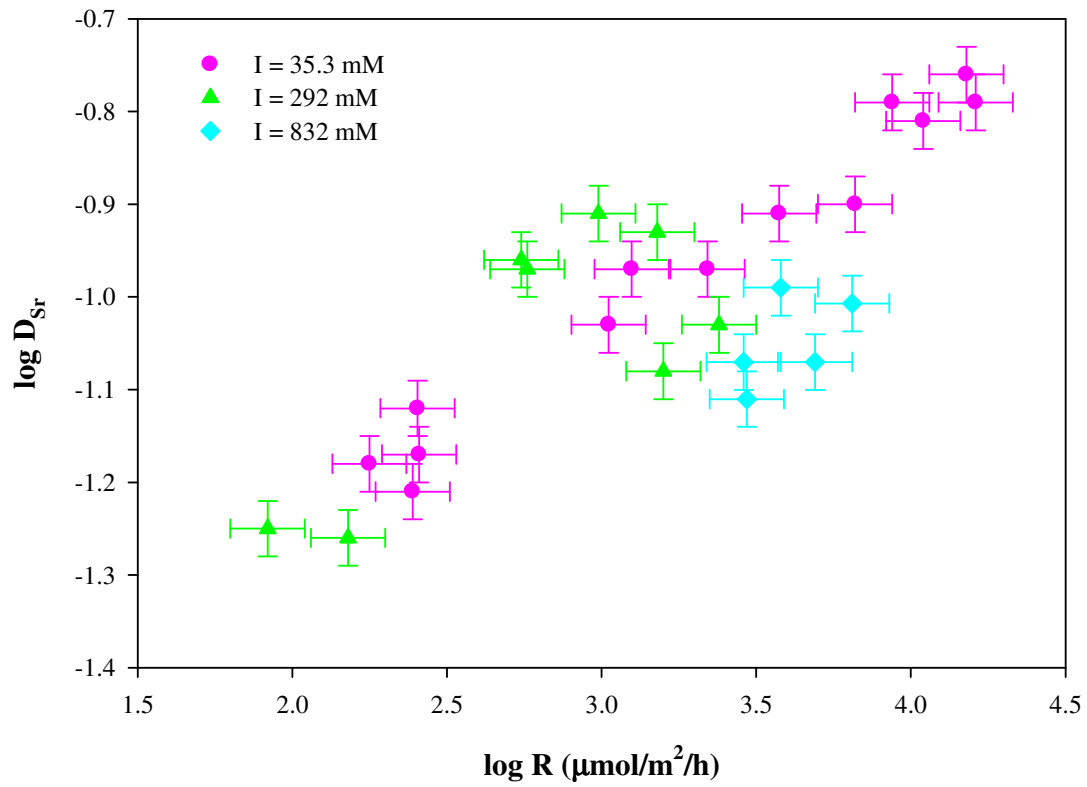
685

686

687

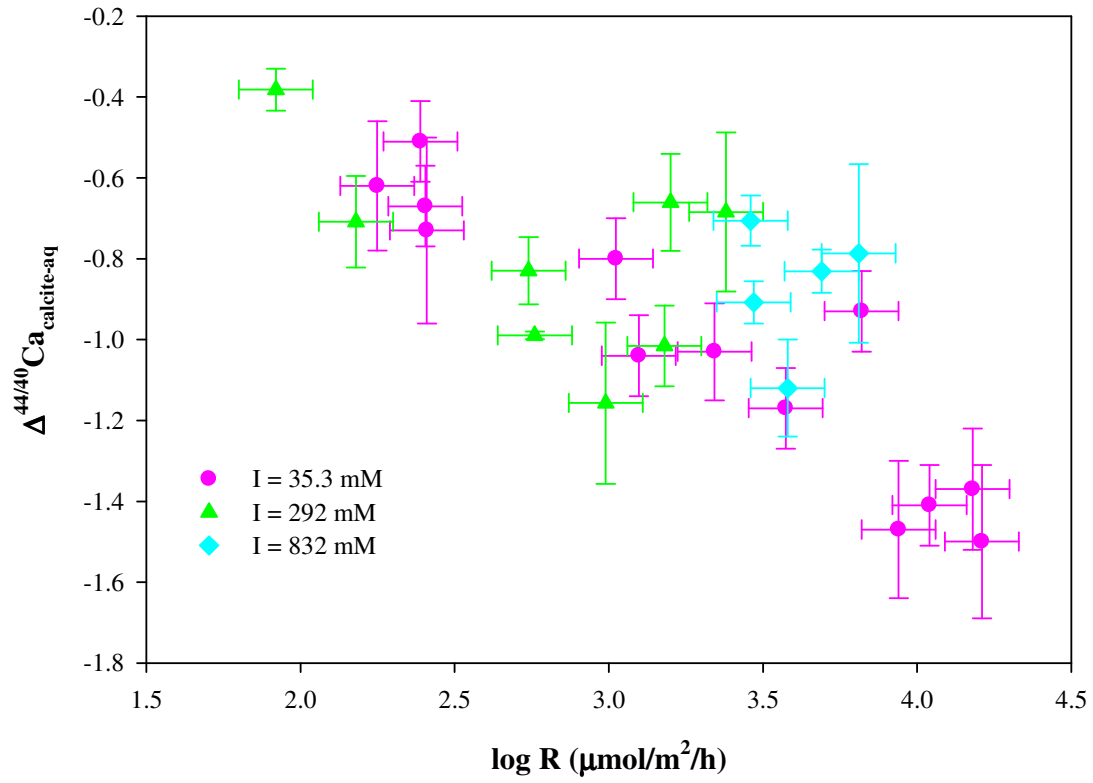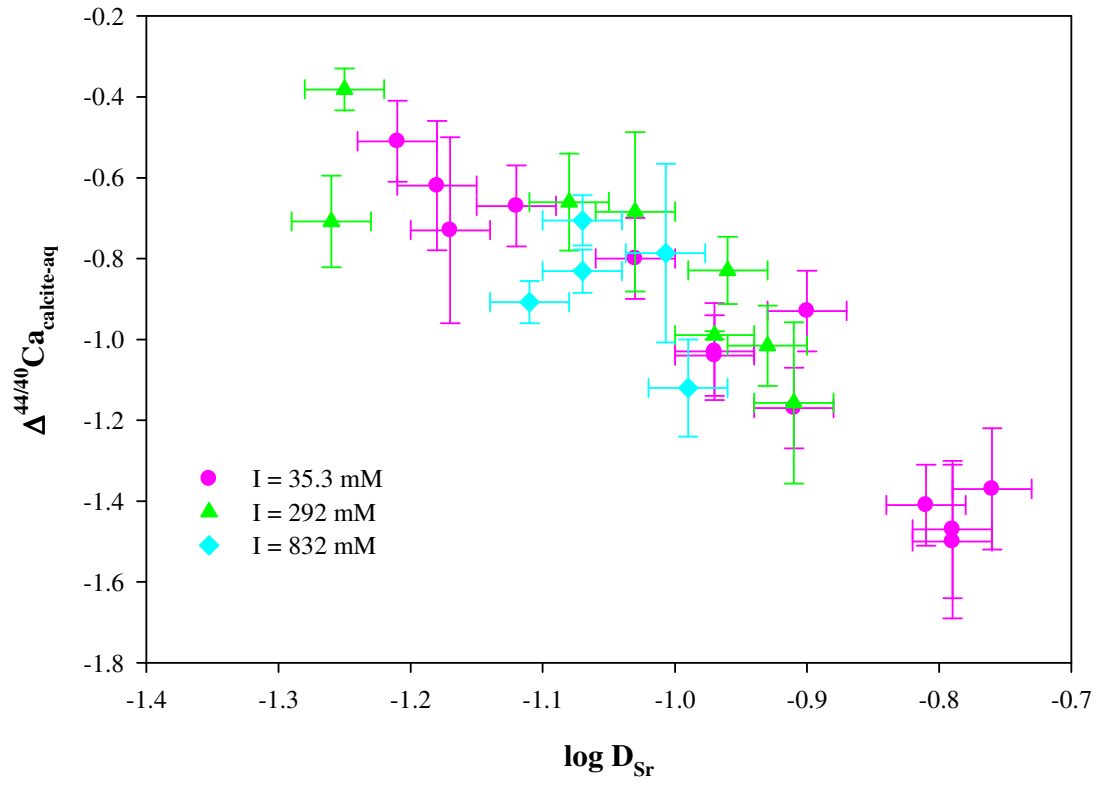688

689

690   Fig. 1

691

692

693   Fig. 2

694

695

696

697

698

704 Fig. 4

705

706

707

708

709

710

711